Available online at www.sciencedirect.com
ScienceDirect
Journal of Power Sources 168 (2007) 447–452
JOURNAL OF POWER SOURCES
www.elsevier.com/locate/jpowsour

Short communication

Comparison of infiltrated ceramic fiber paper and mica base compressive seals for planar solid oxide fuel cells

Shiru Le [a], Kening Sun [a,*], Naiqing Zhang [a,b], Yanbin Shao [a], Maozhong An [a], Qiang Fu [a], Xiaodong Zhu [a]

[a] *Department of Applied Chemistry, Harbin Institute of Technology, No. 92 of West Dazhi Street, P.O. Box 211, Harbin 150001, China*
[b] *The Research Station on Material Science and Engineering for Postoral Fellows, No. 2 Yikang Street, Harbin 150001, China*

Received 6 February 2007; received in revised form 5 March 2007; accepted 6 March 2007
Available online 12 March 2007

Abstract

Solid oxide fuel cells using non-glass sealants have become increasingly common. In this paper, fumed silica infiltrated ceramic fiber paper with pre-compression was compared with plain and pre-compressed at 10 MPa hybrid mica as compressive seals. Leakage tests were measured under a 0.1–1.0 MPa compressive load with the pressure gradient varying from 2 to 15 kPa. The results demonstrated that the leakage rate of infiltrated fiber paper was 0.04 sccm cm^{-1} for a 10 kPa gradient, under 1.0 MPa compressive load, while for mica it was 0.60 and 0.63 sccm cm^{-1} which indicated that the infiltrated ceramic fiber paper showed a much lower leakage than mica. Long-term thermal cycling tests demonstrated that although the leakage of fumed silica infiltrated fiber paper was slightly higher than that of hybrid mica, it remained stable after 20 thermal cycles and no interlayer was needed. The mass loss of the fiber paper was 1.7×10^{-2} mg cm^{-2} h^{-1} in a hydrogen environment at 1073 K for 200 h. The leakage of infiltrated fiber paper remained about 0.06 sccm cm^{-1} after reduction.

Keywords: SOFC; Compressive seals; Ceramic fiber; Plain mica; Hybrid mica

1. Introduction

Solid oxide fuel cells (SOFCs) are being developed for a wide range of applications such as automobiles and power generators [1]. Planar SOFCs were the focus of SOFC development as compared to tubular SOFCs [2]. Good brazing between the current collector and the tube can be achieved to avoid leakage in tubular SOFCs [3]. However, sealing has become one of the most important problems which hinder the advancement of planar SOFCs. The seals must be an insulator, stable in both oxygen and hydrogen environments and chemically compatible with the other fuel cell components.

Traditional SOFC seals have focused on rigid glass and glass-ceramics. However, glass-ceramics are disadvantageous for long-term stack operation, and tend to react with the electrodes and interconnects at SOFC operating temperatures. Furthermore, a non-destructive dismantling of stacks is nearly impossible [4].

Compressive seals were developed to overcome the disadvantages of rigid seals. Deformable metallic compressive seals [5,6] and mica base compressive seals were developed [7–12]. The major advantage of compressive seals is that the seals are not rigidly fixed to the other SOFC components, so an exact match of thermal expansion was not required. Deformable superalloys, however, are not suitable for SOFC compressive seals because of the occurrence of short circuits [5,6]. Plain and hybrid mica, with a glass or silver interlayer, was studied for planar SOFC compressive seals.

Ceramic fiber is an insulator made of an alumina–silica composition. It resists oxidation and is easy to fabricate and install with an elastic recovery higher than 93.35% [13]. It can be used for extended periods of time, and is also used in furnace insulation and high temperature gaskets. Most of its characteristics meet the demands for SOFC sealing. However, its porosity is

* Corresponding author. Tel.: +86 451 8641 2153: fax: +86 451 8641 2153.
E-mail address: leshiru2005@yahoo.com.cn (K. Sun).

0378-7753/$ – see front matter © 2007 Elsevier B.V. All rights reserved.
doi:10.1016/j.jpowsour.2007.03.014

higher than 90% and infiltration is required for its application to SOFC sealing to reduce the leak rates. Apart from effectively reducing the leak rates, additionally, the infiltration must be insulating and be chemically stable in the SOFC environment.

In water, fumed silica has a high dispersion and a chain-like particle morphology, forming colloidal silica. The fumed silica bonding together via weak hydrogen bonds forms a three-dimensional network. After drying, colloidal silica with a size much larger than that of fumed silica filled in the voids of the fiber, effectively reducing the leakage. In our previous study [13], fumed silica infiltrated alumina silica fiber paper pre-compressed at 10 MPa for 10 min showed promising results. The leak rates decreased with the increase of the infiltration amount. In this paper, we compared fumed silica infiltrated alumina silica ceramic fiber paper and mica base compressive seals applied to planar SOFC sealing.

2. Experimental methods

Plain and pre-compressed phlogopite and muscovite mica 0.5 mm in thickness were cut to a 4 cm outer diameter and 2 cm inner diameter. The pre-compressive load was 10 MPa for 10 min. Fumed silica infiltrated alumina silica fiber paper was cut to the same size as that of the mica. The infiltration of the fiber paper was reported in detail in Ref. [13].

The samples were placed between an SS430 steel plate and an SS430 column, which was 4 cm in outer diameter and 2 cm in inner diameter with 1 cm in height. Compressive stresses of 0.1–1 MPa were applied to the cylinder. A volume of 150 cm^3 gas reservoir was kept at ambient conditions and connected to the samples via a 1 mm inner diameter SS430 tube. A 15 kPa nitrogen pressure gradient was applied. The line between the nitrogen source and the reservoir was then closed, and the resulting pressure decayed from 15.0 to 2.0 kPa with time, the leak rates were calculated using the equation below.

$$L = \frac{(P_i - P_f)V}{P_f \Delta t C} \quad (1)$$

where L is the leak rate (sccm cm^{-1}, standard cubic centimeter per minute per centimeter), V the sum of the reservoir volume and SS430 steel column pipe (159.42 cm^3) and P is the pressure. Subscripts i and f represent the initial and final conditions, and C is the outer length of the SS430 cylinder circumference (12.56 cm).

To evaluate the stability of the infiltrated fiber paper in oxidizing and reducing environments, long-term stability of the samples with the size of 4 cm in outer diameter and 2 cm in inter diameter in air and hydrogen environments were conducted. The samples were heated from room temperature to 1073 K in 150 min, situated at 1073 K for 120 min for the leakage test and then cooled to room temperature in 240 min. The temperature profile for the thermal cycling is shown in Fig. 1. The infiltrated ceramic fiber paper in hydrogen environment at the flow rate of 50 sccm at 1073 K was reduced for 50 h, and the leak rate after reduction was measured.

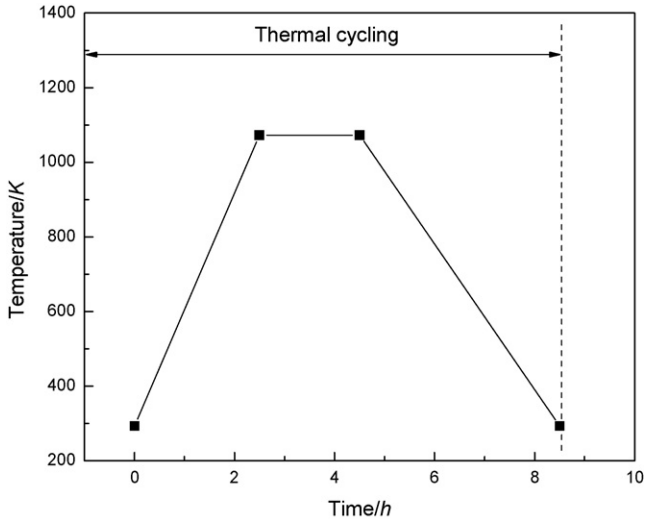

Fig. 1. Temperature profile for thermal cycling.

The morphology of the samples was observed by scanning electron microscopy with a HITACHI S4700. Optical micrographs of the SS430 column and SS430 steel plate were obtained.

3. Results and discussion

3.1. Comparing infiltrated ceramic fiber paper and plain mica

The results of a leakage test for fumed silica infiltrated ceramic fiber paper and plain phlogopite and muscovite mica are listed in Table 1. The leak rates of all samples decreased with increase of compressive load. There are two possible paths for leaks [7,12,13]: one is through the seals itself; the other is through the interfaces between the seals and the steel plate or the seals and the column. Higher compressive load made for closer contact between the mica and fiber paper, thus reducing the leakage through the seals itself. Also, higher compressive loads make a more hermetic seal between the interfaces, thereby leading to a decrease of leakage. For infiltrated ceramic fiber paper at a 15 kPa pressure gradient and 0.1 MPa compressive load, the leakage rate was 0.16 sccm cm^{-1}, which was reduced to 0.05 sccm cm^{-1} at 1.0 MPa, i.e. reduced by about three-fold. For phlogopite and muscovite mica, it was 1.24 and 1.18 sccm cm^{-1} at 0.1 MPa, respectively, but decreased to 0.88 and 0.93 sccm cm^{-1} at 1.0 MPa. We also found that the pre-compression at 10 MPa for mica showed litter improvement of sealing characteristics. At a 1.0 MPa compressive load and a 10 kPa pressure gradient, the leakage of muscovite and phlogopite mica without pre-compression was 0.64 and 0.66 sccm cm^{-1}, respectively, but that was 0.60 and 0.58 sccm cm^{-1}, respectively, for muscovite and phlogopite mica pre-compressed at 10 MPa for 10 min.

Looking in Table 1, one can note that the infiltrated fiber paper showed much better sealing characteristics than muscovite and phlogopite mica. At a 10 kPa pressure gradient and 1.0 MPa, the

Table 1
Leak rates for compressive stress 0.1–1 MPa and gauge pressure 3–15 kPa

	Pressure gauge (kPa)			
	15	10	5	3
Fumed silica infiltrated fiber paper				
0.1 MPa	0.16	0.11	0.05	0.03
0.2 MPa	0.13	0.08	0.03	0.02
0.4 MPa	0.08	0.05	0.03	0.01
0.8 MPa	0.07	0.04	0.02	a
1.0 MPa	0.05	0.04	0.01	a
Muscovite mica				
0.1 MPa	1.24	0.90	0.51	0.23
0.2 MPa	1.16	0.85	0.46	0.21
0.4 MPa	1.06	0.77	0.40	0.19
0.8 MPa	0.95	0.69	0.37	0.17
1.0 MPa	0.88	0.64	0.32	0.16
Muscovite mica pre-pressed at 10 MPa				
0.1 MPa	1.08	0.78	0.42	0.20
0.2 MPa	1.02	0.72	0.38	0.19
0.4 MPa	0.95	0.68	0.38	0.18
0.8 MPa	0.87	0.62	0.34	0.15
1.0 MPa	0.82	0.60	0.29	0.15
Phlogopite mica				
0.1 MPa	1.18	0.82	0.48	0.22
0.2 MPa	1.11	0.77	0.44	0.21
0.4 MPa	1.03	0.72	0.39	0.20
0.8 MPa	0.95	0.66	0.37	0.16
1.0 MPa	0.93	0.66	0.30	0.15
Phlogopite mica pre-pressed at 10 MPa				
0.1 MPa	1.14	0.82	0.45	0.22
0.2 MPa	1.06	0.77	0.42	0.20
0.4 MPa	0.98	0.70	0.38	0.19
0.8 MPa	0.89	0.63	0.34	0.16
1.0 MPa	0.82	0.58	0.30	0.14

a, Lower detected limit.

leakage rate was 0.04 sccm cm^{-1} for infiltrated fiber paper, while it was 0.64 and 0.66 sccm cm^{-1}, respectively, for muscovite and phlogopite mica. This can also be seen in Fig. 2—the leakage of infiltrated ceramic fiber paper was much lower than that of mica under the same compressive load. The leak rates of mica were about 15 times than that of infiltrated fiber paper at the 1.0 MPa, with a 10 kPa pressure gradient.

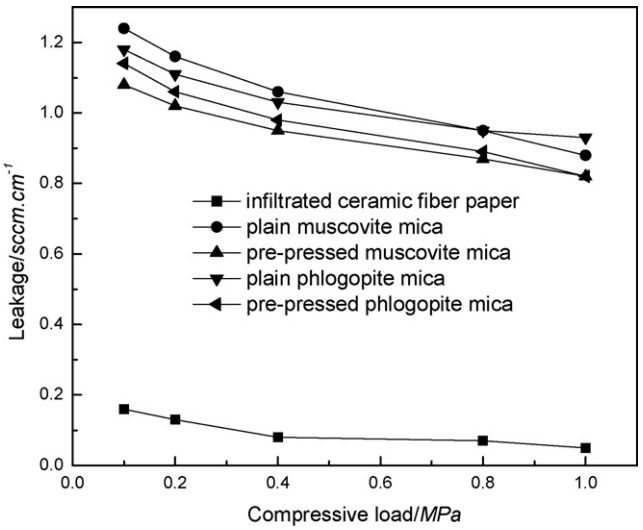

Fig. 2. Effect of compressive load to leak rates (tested at a 15 kPa pressure gradient).

The cross-sectional SEM images of the samples are shown in Fig. 3. There is little difference between the phlogopite mica and muscovite mica, both composed of mica sheet, leaving a space between each mica sheet as large as 3 μm. Gas leakage occurred through these open fissures. Unlike the layer structure of mica, however, the fumed silica infiltrated alumina silica fiber compacted closely under a 10 MPa pre-compressive high load and holes in the infiltrated fiber paper cross-section were not evident. Many cracks between the colloidal silica disappeared under 10 MPa pre-compression [13]. Thus, leakage across the fiber paper interior sealant is lower than that of mica.

Another possible leakage occurred between the interfaces. These are related to the surface characteristics of the seals, steel and column. Many defects were found in the steel plate and steel column optical micrograph in Fig. 4, including long grooves and irregular grooves, especially when the surface was ground with abrasive paper. The SEM images of the sealant surface after testing are shown in Fig. 5. The surfaces of muscovite and phlogopite mica paper were rough after testing. This is because the mica is composed of many small mica platelets randomly pressed together. When the rough surfaces were pressed on the

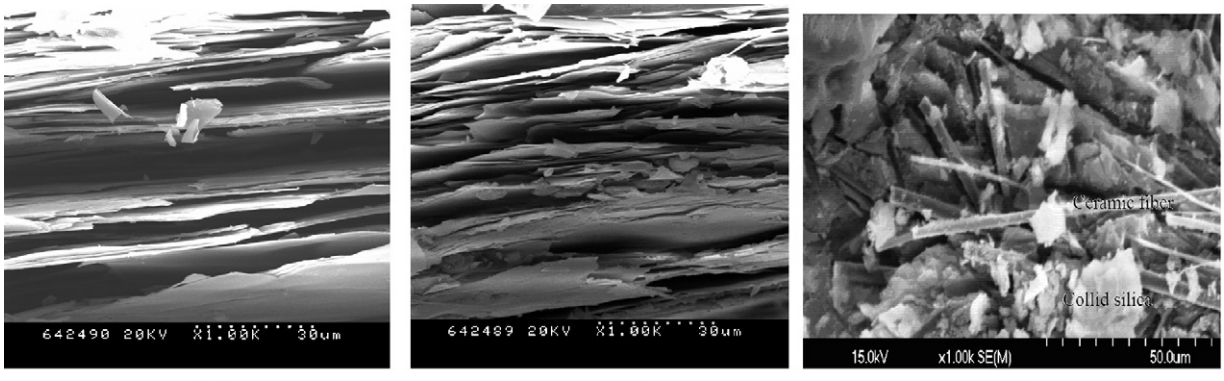

Fig. 3. Cross-sectional SEM images of: (a) phlogopite mica, (b) muscovite mica and (c) infiltrated fiber paper.

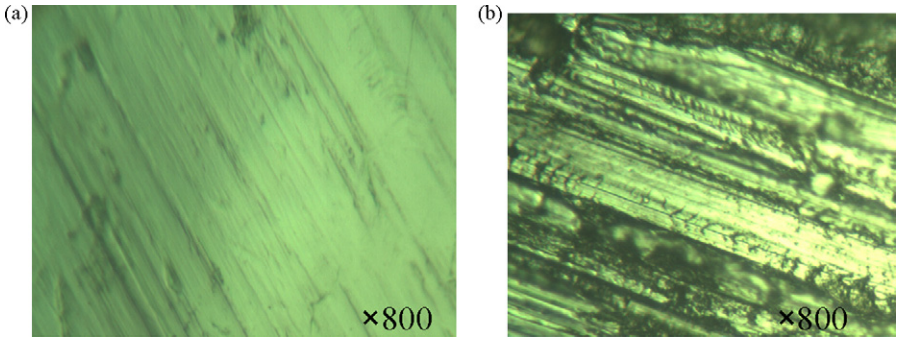

Fig. 4. Optical micrograph showing the surface morphology of: (a) SS430 steel plate and (b) SS430 steel column which was ground with a #120 grit paper.

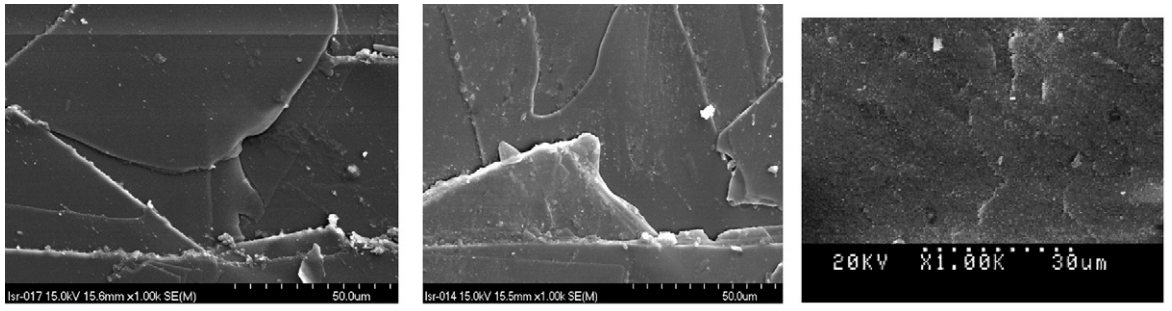

Fig. 5. SEM image of the sealing material surface after testing.

groove steel surface, the mica could not fill the interfacial space, and this produced high leakage across these interfaces between the seals and steel plate and the interface between the seals and the steel column. But the surface of the infiltrated ceramic fiber paper was much smoother than that of mica. Most importantly, the surface was covered by flat colloidal silica. The reason was that fumed silica formed colloidal silica after dispersion in water. Large amounts of colloidal silica distributed on the ceramic fiber surface changed its shape easily at high compressive loads. At a 10 MPa pre-compressive load, the colloidal silica on the surface not only covered the irregular fiber but also filled the grooves of the surface; thus greatly reducing the leakage.

3.2. Comparing infiltrated ceramic fiber with hybrid mica

Plain and pre-compressed mica showed poor sealing characteristics, so hybrid mica compressive seals were developed [7–12], using silver and glass interlayers. The leakage of mica seals with silver or glass interlayers was tested at about 0.7 MPa (100 psi) and a 14 kPa pressure gradient [12]. The infiltrated fiber paper was measured at 0.8 MPa and a 15 kPa pressure gradient was used.

It can be seen in Fig. 6 that the leakage of infiltrated fiber paper was stable at about 0.06 sccm cm^{-1}, showing little or no change over 20 thermal cycles. The SEM cross-sections and surface images of the infiltrated fiber paper after the thermal cycles are shown in Fig. 7. It is seen that the fumed silica and fiber paper remain closely compacted, and the surface of the fiber paper after the thermal cycles was smooth. The smooth fumed silica filled the small spaces in the interface. For hybrid mica seals, the initial leak rates of mica with silver and glass interlayers were lower than 0.01 sccm cm^{-1}. However, the sealing performance degraded with thermal cycling due to fragmentation and particle formation occurring along the grain boundaries [12]. It also increased with thermal cycling of mica based glass interlayers. This may be due to indentation and fragmentation damage that occurred in the mica [12]. The cause of indentations was attributed to the roughness of the contact surface, and the fragmentations can be attributed to the residual stresses at indentations where the mica was mechanically interlocked with the mating surfaces. Though the leakage of the infiltrated fiber paper was slightly higher than that of the hybrid mica

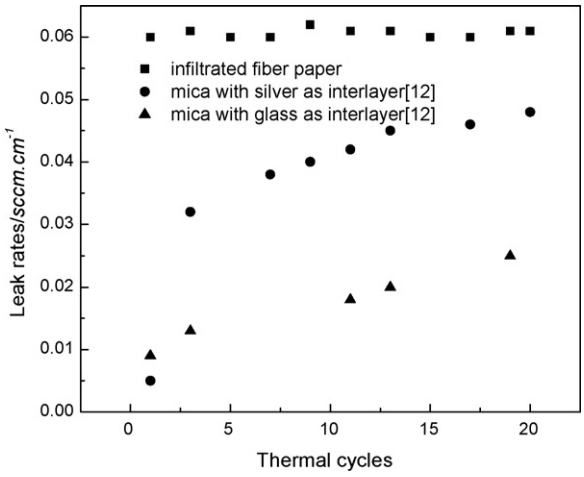

Fig. 6. Effect of thermal cycle of the sealant.

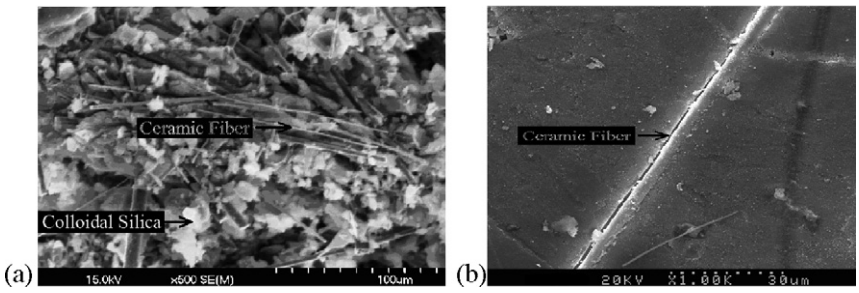

Fig. 7. The (a) cross-sectional (b) surface SEM image of infiltrated fiber paper after thermal cycles.

with glass interlayer, no glass or silver interlayer was required in infiltrated fiber paper sealing. This will hopefully reduce to the cost of SOFC fabrication. Moreover, no glass interlayer would make replacement of functional components much easier.

3.3. Weight loss in a reducing environment

Quadrivalent silicon will form $Si(OH)_4$ in a reducing environment, so there is concern as to whether fumed silica infiltrated fiber paper and mica are stable in a hydrogen environment.

Fig. 8 shows the mass loss of infiltrated fiber paper and plain mica in a hydrogen environment at 1073 K for 200 h. The mass loss of the infiltrated fiber paper was 1.7×10^{-2} mg cm^{-2} h^{-1}, much higher than that of phlogopite and muscovite mica, which was 1.3×10^{-4} mg cm^{-4} h^{-1} and 1.6×10^{-4} mg cm^{-2} h^{-1}, respectively. The reason is that there was much higher silicon element content in the fumed silica infiltrated fiber paper. The silicon content was 75.5% in 100 wt% fumed silica infiltrated fiber paper [13], but only about 20.15% in mica. However, a 1.7×10^{-2} mg cm^{-2} h^{-1} mass loss for the SOFC seals is low. This is only 0.017 g cm^{-2} for 1000 h operation. The leak rate after hydrogen reduction is shown in Fig. 9. It was 0.06 sccm cm^{-1} at 0.8 MPa and a 15 kPa pressure gradient. This demonstrates that there was nearly no influence of hydrogen reduction on the infiltrated fiber paper seals.

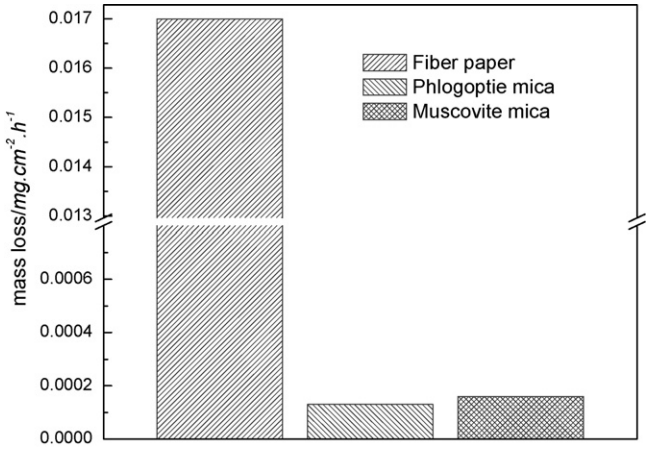

Fig. 8. Mass loss of seals in hydrogen environment (tested at 1073 K in hydrogen environment with flow rate 50 sccm).

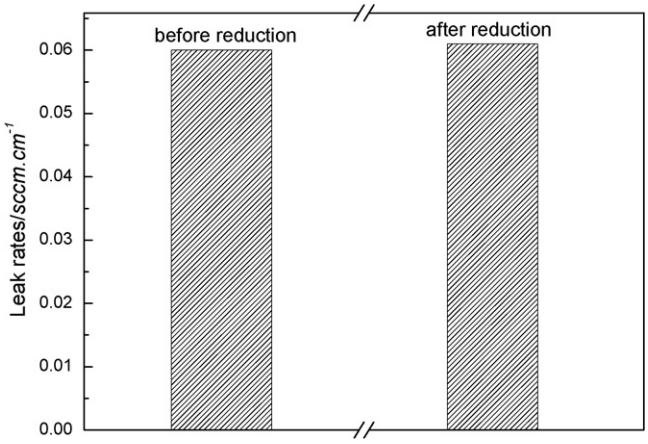

Fig. 9. Leak rates of fiber paper before and after reduction (tested at 0.8 MPa, 15 kPa pressure gradient).

3.4. Estimation of total fuel loss

To estimate the leakage when using these seals in an SOFC stack, we assume that the active area of each cell is $8 \times 8 = 64$ cm^2 with the outer seal length of $4 \times 15 = 60$ cm per cell. The operating current density of 0.7 A cm^{-2} needed a fuel flow rate of 470 sccm. Considering fuel utilization of 80%, a 584 sccm of fuel flow rate was required. If 15 kPa (15 kPa is much higher than a real SOFC fuel pressure across the seals) 0.8 MPa compressive load was applied, the leak rate is 0.06 sccm cm^{-1}, then the total leakage is only 0.6%, which is acceptable for SOFC sealing requirement.

4. Conclusions

The leakage rate of the infiltrated fiber paper was 0.04 sccm cm^{-1} at a 1.0 MPa compressive load and a 10 kPa pressure gradient. The leakage was 0.64 and 0.66 sccm cm^{-1} for plain muscovite and phlogopite mica, and was 0.60 and 0.58 sccm cm^{-1} for pre-compressed muscovite and phlogopite mica. This work demonstrated that infiltrated fiber paper showed a much better sealing characteristic than plain mica. Thermal cycling tests demonstrated that leakage through infiltrated fiber paper remained about 0.06 sccm cm^{-1} at 0.8 MPa and a 15 kPa pressure gradient after 20 cycles. Though it was slightly higher than that of hybrid mica with silver and glass as interlayer, no interlayer is required using infiltrated fiber paper sealing. 0.06 sccm cm^{-1} is acceptable for SOFC sealing. The mass loss

of the infiltrated fiber paper in a hydrogen environment was 1.7×10^{-2} mg cm^{-2} h^{-1} at 1073 K for 200 h, which was higher than that of mica, but the reduction had an insignificant influence on the leakage rates.

Acknowledgement

This project is financially supported by the National Natural Science Foundation of China (No. 9051006).

References

[1] F.J. Gardner, M.J. Day, N.P. Brandon, M.N. Pashley, M. Cassidy, J. Power Sources 86 (2000) 122–129.
[2] N.Q. Minh, Solid State Ionics 174 (2004) 271–277.
[3] N.M. Summes, Y. Du, R. Bove, J. Power Sources 145 (2005) 428–434; W.F. Jefrey, J. Power Sources 147 (2005) 46–57.
[4] M. Bram, S. Reckers, P. Drinovac, J. Monch, R.W. Steinbrech, H.P. Buchkremer, D. Stover, Electrochem. Soc. Proc. 8 (2003) 889–897.
[5] M. Bram, S. Rechers, P. Drinovac, J. Monch, R.W. Steinbrech, H.P. Buchkremer, D. Stover, J. Power Sources 138 (2004) 111–119.
[6] S.P. Simner, J.W. Stevenson, J. Power Sources 102 (2001) 310–316.
[7] Y.-S. Chou, J.W. Stevenson, J. Power Sources 135 (2004) 72–78.
[8] Y.-S. Chou, J.W. Stevenson, J. Power Sources 124 (2003) 473–478.
[9] Y.-S. Chou, J.W. Stevenson, J. Power Sources 112 (2002) 130–136.
[10] Y.-S. Chou, J.W. Stevenson, J. Power Sources 115 (2003) 274–278.
[11] Y.S. Chou, J.W. Stevesnon, J. Am. Ceram. Soc. 86 (6) (2003) 1003–1007.
[12] Y.-S. Chou, J.W. Stevenson, L.A. Chick, J. Mater. Res. 18 (2003) 2243–2250.
[13] S. Le, K. Sun, N. Zhang, J. Power Sources 161 (2006) 901–906.